ISSN 0006-2979, Biochemistry (Moscow), 2008, Vol. 73, No. 8, pp. 897-905. © Pleiades Publishing, Ltd., 2008.
Published in Russian in Biokhimiya, 2008, Vol. 73, No. 8, pp. 1114-1123.
Originally published in Biochemistry (Moscow) On-Line Papers in Press, as Manuscript BM07-434, May 18, 2008.

Metal Cofactors Play a Dual Role in *Mycobacterium tuberculosis* Inorganic Pyrophosphatase

E. V. Rodina[1,2]*, L. P. Vainonen[1], N. N. Vorobyeva[1], S. A. Kurilova[2], T. S. Sitnik[2], and T. I. Nazarova[2]

[1]*Chemical Faculty, Lomonosov Moscow State University, 119992 Moscow, Russia; fax: (495) 932-8846; E-mail: rodina@belozersky.msu.ru*
[2]*Belozersky Institute of Physico-Chemical Biology, Lomonosov Moscow State University, 119992 Moscow, Russia; fax: (495) 939-3181; E-mail: nazarova@belozersky.msu.ru*

Received December 25, 2007
Revision received January 24, 2008

Abstract—Inorganic pyrophosphatase from *Mycobacterium tuberculosis* (Mt-PPase) is one of the possible targets for the rational design of anti-tuberculosis agents. In this paper, functional properties of this enzyme are characterized in the presence of the most effective activators—Mg^{2+} and Mn^{2+}. Dissociation constants of Mt-PPase complexed with Mg^{2+} or Mn^{2+} are essentially similar to those of *Escherichia coli* PPase. Stability of a hexameric form of Mt-PPase has been characterized as a function of pH both for the metal-free enzyme and for Mg^{2+}- or Mn^{2+}-enzyme. Hexameric metal-free Mt-PPase has been shown to dissociate, forming monomers at pH below 4 or trimers at pH from 8 to 10. Mg^{2+} or Mn^{2+} shift the hexamer–trimer equilibrium found for the apo-Mt-PPase at pH 8-10 toward the hexameric form by stabilizing intertrimeric contacts. The pK_a values have been determined for groups that control the observed hexamer–monomer (pK_a 5.4), hexamer–trimer (pK_a 7.5), and trimer–monomer (pK_a 9.8) transitions. Our results demonstrate that due to the non-conservative amino acid residues His21 and His86 in the active site of Mt-PPase, substrate specificity of this enzyme, in contrast to other typical PPases, does not depend on the nature of the metal cofactor.

DOI: 10.1134/S0006297908080075

Key words: pyrophosphatase, *M. tuberculosis*, Mg^{2+}, Mn^{2+}, metal cofactor, cofactor specificity

Mycobacterium tuberculosis is a causative agent of human tuberculosis. Despite the wide use of vaccines and antibiotics, this hard-to-treat disease remains one of the most ubiquitous infectious diseases [1-3]. Rational design of new anti-tuberculosis agents requires knowing and analysis of the spatial structures of key proteins produced by *M. tuberculosis*. To solve this problem, the joint *Mycobacterium tuberculosis* Structural Genomics Consortium was created in 2001, which now includes 430 participants from 15 countries [3]. Up to now, the structures of more than 200 proteins of this bacterium, including soluble inorganic pyrophosphatase [4], have been characterized as possible targets for anti-tuberculosis therapy.

Inorganic pyrophosphatases (PPases, EC 3.6.1.1) catalyze hydrolysis of inorganic pyrophosphate (PP_i) forming two phosphate ions. Hydrolysis of PP_i is a necessary step for important cell pathways to proceed, including biosynthesis of proteins and nucleic acids, which makes PPases key enzymes for any living organisms.

Soluble PPases can be divided into two non-homologous families, I and II. Family I PPases are more numerous and they are well-characterized enzymes produced by both eukaryotes and prokaryotes. Family II PPases have only recently been discovered. They have been found in 109 bacterial species, many of which are human pathogens. Four prokaryotic species from the order *Vibrionales* contain genes for both family I and family II PPases [5].

For both PPase families, enzymatic activity is metal-dependent, at least three ions of metal-cofactor being involved in catalysis. Two M^{2+} occupy binding sites M1 and M2 in the active site of the free enzyme, thus forming the holoenzyme molecule EM_2. The third metal ion occupies the M3 site as a part of substrate molecule $MP_2O_7^{2-}$. The active site also has a fourth metal binding

Abbreviations: E-PPase) *Escherichia coli* inorganic pyrophosphatase; Mt-PPase) *Mycobacterium tuberculosis* inorganic pyrophosphatase; PNP) imidodiphosphate.

* To whom correspondence should be addressed.

site M4, but its occupation in the excess of metal cofactor causes the inhibition of enzymatic activity. Either Mg^{2+} or Mn^{2+} can act as PPase cofactor, their relative activating efficiency being the key factor that distinguishes family I from family II enzymes. Family I PPases are activated most efficiently by Mg^{2+}, while their Mn^{2+}-supported activity is two orders of magnitude lower [6, 7]. Quite the contrary, family II PPases prefer Mn^{2+} as a cofactor and are 20 times less active when Mg^{2+}-activated [8, 9]. This difference in cofactor specificity of PPases is assumed to be due to the protein ligands binding the metal cofactor ions. In family I PPases, metal ions are liganded by the carboxylic groups of invariant Asp and Glu residues. In family II enzymes, there are three His residues in the active site, two of which make direct contacts to the metal ions, thus determining the very high affinity of these PPases to Mn^{2+}.

In this work, we have studied *M. tuberculosis* PPase (Mt-PPase), which belongs to family I. Like any other prokaryotic enzyme of this family, the molecule of Mt-PPase is a homohexamer. Each subunit of 168 amino acid residues has a mass of about 20 kD [4]. For the family I PPases, the active site is known to be highly evolutionarily conservative, all polar residues being identical in all known PPases. Despite that, Mt-PPase as well as PPase from the close relative *Mycobacterium leprae* has a unique feature. There are two histidine residues in its active site, His21 and His86, absent in all other PPases. In the PPase from *E. coli* (E-PPase), the corresponding amino acid residues Lys34 and Ala99 are located near the metal binding sites M4 and M3, respectively. This feature, which makes Mt-PPase structurally similar to family II PPases, may influence cofactor specificity of this enzyme.

In the only paper published on Mt-PPase crystal structure, the metal-free form is described and some functional characteristics of this enzyme are given [4]. According to these data, Mt-PPase is most efficiently activated by Mg^{2+}, like the other family I enzymes. It should be noted though that the characteristics given in [4] were determined for the preparation of Mt-PPase tagged at the N-terminus with additional histidine residues (6His-Mt-PPase). Since this additional sequence was not seen on the electron density map and so it was not included in the structure, it is hardly possible to make any conclusions as to its conformation and its location with respect to the rest of the molecule. On the other hand, every imidazole group may be a good ligand for complexing a metal ion, so this insertion may form an additional metal binding site, thus affecting some metal-dependent properties of the enzyme.

In order to avoid the possible influence of a histidine insertion upon the enzymatic activity and other properties, in this work we obtained a preparation of Mt-PPase without any insertions. For this preparation, the functional characteristics were determined in the presence of Mg^{2+} or Mn^{2+} as cofactors. The properties investigated were Mg^{2+}- or Mn^{2+}-supported hydrolysis of PP_i, ATP, and imidodiphosphate (PNP); dissociation constants of Mt-PPase complexed with these cofactors at the sites M2 and M4; and the influence of Mg^{2+} or Mn^{2+} on the stability of the hexameric form of Mt-PPase. Based on our results, we suppose that neither His21 nor His86 are the direct ligands of the metal cofactor ions, but they affect greatly the microenvironment of the catalytic groups. We also found that both Mg^{2+} and Mn^{2+} are able to shift the hexamer–trimer equilibrium of Mt-PPase toward the hexameric form by stabilizing intertrimeric contacts.

MATERIALS AND METHODS

Chemicals. The chemicals used in the study were purchased in high-purity grade from Sigma (USA), Fluka (Switzerland), Serva (Germany), Merck (Germany), or Pharmacia Fine Chemicals (Sweden). All stock solutions were freshly prepared with deionized water additionally purified with MilliQ. Recombinant *E. coli* PPase was isolated and purified as described in [10].

Plasmid construction for expression of *M. tuberculosis* PPase without additional insertions. A modified plasmid pET-28a, which contained the gene of *M. tuberculosis* PPase with the N-terminal six-histidine tag, was used as an original vector. Two oligonucleotides were synthesized complementary to the 3′- and 5′-ends of the plasmid sequence corresponding to the PPase gene with its regulatory regions. Restriction sites *Nde*I or *Eco*RI were included in the oligonucleotides, respectively. The fragment containing the full-size gene of untagged Mt-PPase and these restriction sites was obtained using PCR and then cloned to the *Nde*I-*Eco*RI sites of pET-23a. The ligase mixture was used to transform *E. coli* strain XL-I, and the resulting clones were tested for the size of plasmid DNA. Four clones that carried an insertion at the restriction sites *Nde*I-*Eco*RI and had similar expression level of PPase were used in subsequent experiments.

Isolation and purification of *M. tuberculosis* PPase. Recombinant plasmid containing the gene of untagged Mt-PPase was transformed into *E. coli* C-41(DE3). A cell culture was grown at 37°C for about 3 h to an optical density of 0.6, induced by the addition of isopropyl-β-D-thiogalactopyranoside (IPTG) to a concentration of 1 mM, and then grown for another 3 h. After lysis by lysozyme with the addition of phenylmethylsulfonyl fluoride (PMSF) and centrifugation, streptomycin was added to the supernatant to precipitate nucleic acids, and the mixture was recentrifuged to remove debris. The supernatant was incubated for 5 min at 65°C, followed by recentrifugation to remove denatured protein impurities. Ammonium sulfate was added to the supernatant. After centrifugation, the sediment containing the target protein was dissolved in 50 mM Tris-HCl, pH 7.5, with 2 mM

$MgCl_2$. The protein solution was gel filtered on a column with Sephadex G-50 equilibrated with the same buffer to remove ammonium sulfate, and then purified on a column with DEAE-Sepharose equilibrated with the same buffer, adding NaCl in three steps from 0.1 to 0.3 M. Mt-PPase was eluted at 0.3 M NaCl. The yield of Mt-PPase was 60 mg from 3 liters of cell culture. The purity of protein preparations as characterized by polyacrylamide gel electrophoresis was 98-99%.

Protein preparations were stored as suspensions with $(NH_4)_2SO_4$ and desalted immediately before use by gel filtration on a column with Sephadex G-50 (fine) equilibrated with 50 mM Tris-HCl, pH 7.5, with elution by the same buffer. Mt-PPase was additionally incubated for 24 h with 50 μM EDTA, which was then removed by centrifugation on a spin column with Sephadex G-50 (fine) equilibrated with the same buffer. The concentration of the enzyme solutions was determined by UV-spectrophotometry using the values A_{280} of 1.18 and 0.98 (for protein solutions with 1 mg/ml concentration) for E-PPase and Mt-PPase, respectively [4, 11].

Kinetic measurements. Hydrolytic activity of PPases was determined at 25°C by the rate of P_i release using a semi-automatic phosphate analyzer [12]. Total concentrations of MCl_2 and $Na_4P_2O_7{\cdot}10H_2O$ were calculated using the following values of dissociation constants (K_d) for MPP_i and M_2PP_i [13]: for the magnesium complexes, 0.70 and 16.23 mM at pH 6.0; 47.7 μM and 2.42 mM at pH 7.5; 2.93 μM and 2.01 mM at pH 9.0; for the manganese complexes, 23 μM and 0.13 mM at pH 7.5.

Kinetic parameters of Mg^{2+}-supported hydrolysis of PP_i by Mt-PPase were determined in 50 mM buffer (MES-NaOH, pH 6.0; Tris-HCl, pH 7.5 or 9.0), at 2 mM Mg^{2+} and 3-500 μM $MgPP_i$. Kinetic parameters of Mn^{2+}-supported hydrolysis were determined in 50 mM Tris-HCl, pH 7.5, at 200 μM Mn^{2+} and 1-30 μM $MnPP_i$.

The rates of hydrolysis of ATP and PNP were determined in 50 mM Tris-HCl, pH 7.5, by measuring phosphate accumulated in the reaction mixture. In the case of ATP, reaction mixture of total volume 2 ml contained 7.5 μM enzyme, cofactor (2 mM Mg^{2+} or 50 μM Mn^{2+}), and substrate (0.3 mM MgATP or MnATP). In the case of PNP, the reaction mixture contained 2.8-3.5 μM enzyme, cofactor (1 mM Mg^{2+} or 50 μM Mn^{2+}), and substrate (0.1 mM MgPNP or MnPNP). The reaction was initiated by addition of enzyme, and after certain time intervals the concentration of P_i was determined in the 200 μl aliquots using a sensitive procedure with the dye malachite green [14].

The rates of hydrolysis of PP_i as a function of metal cofactor concentration were determined in 50 mM Tris-HCl, pH 7.5, at 50 μM $MgPP_i$ and 0.03-10 mM Mg^{2+} (for Mg^{2+}-supported hydrolysis), or at 50 μM $MnPP_i$ and 1-300 μM Mn^{2+} (for Mn^{2+}-supported hydrolysis). Parameters of this dependence were determined as the best fit to Eq. (1):

$$A = \frac{A_0 \cdot [M^{2+}]}{K_d(M2) + [M^{2+}] + \dfrac{[M^{2+}]^2}{K_d(M4)}}, \qquad (1)$$

where $[M^{2+}]$ is concentration of a metal cofactor, K_d(M2) and K_d(M4) are dissociation constants of the complexes enzyme–cofactor metal ion bound at site M2 or M4, respectively, and A_0 is maximum level of enzyme activity without inhibition.

Stability of hexameric Mt-PPase. Enzyme (0.13 mg/ml) was incubated for 2 h at 20°C in 0.05 M buffer solution of fixed pH in the range 3.5-11.0 containing 2 mM Mg^{2+}, or 100 μM Mn^{2+}, or 50 μM EDTA. Buffers used (0.05 M) were: citrate buffer, pH 3.5-5.5; MES-NaOH, pH 6.0-6.5; Tris-HCl, pH 7.0-9.0; N-cyclohexyl-2-hydroxy-3-aminopropanesulfonic acid (CAPSO), pH 10.0-10.5; N-cyclohexyl-3-aminopropanesulfonic acid (CAPS), pH 11.0. After incubation, an aliquot of the mixture was added to 10 ml of 50 mM Tris-HCl, pH 7.5, containing 2 mM Mg^{2+} and 50 μM $MgPP_i$, and PPase activity was determined. Parameters of pH-dependence were determined as the best fit of data to Eq. (2):

$$A = \frac{A_{max}}{1 + 10^{m(pK_a(1) - pH)} + 10^{m(pH - pK_a(2))}}, \qquad (2)$$

where A_{max} is maximum specific activity of a corresponding oligomeric form of enzyme, $pK_a(1)$ and $pK_a(2)$ are acidity constants of the protein groups controlling the stability of the corresponding oligomeric form at the acid and basic pH ranges, respectively, and m is number of protons controlling the stability.

In the case of an apo-form of Mt-PPase, data were fitted to a sum of two pH-dependences for the hexameric and trimeric forms of enzyme. For simplicity, trimeric form was assumed to have $pK_a(1) = 7$ and $m = 1$, and the remaining parameters were determined as the best fit.

Sedimentation analysis. Velocity sedimentation of the solutions of Mt-PPase in 0.1 M buffers was carried out at 20°C using a Spinco E analytical ultracentrifuge (Beckman, USA) (48,000 rpm, scanning at 280 nm). Buffers used were: citrate buffer, pH 4.0; Tris-HCl, pH 7.0; CAPSO, pH 10.0. Enzyme concentration was 5-17 μM. Sedimentation coefficient was calculated as the average from at least three independent experiments.

RESULTS AND DISCUSSION

The interaction between PPases and their cofactor metal ions determines the key characteristics of these enzymes: catalytic activity, stability of their globular structures, oligomeric equilibria, etc. Binding of metal

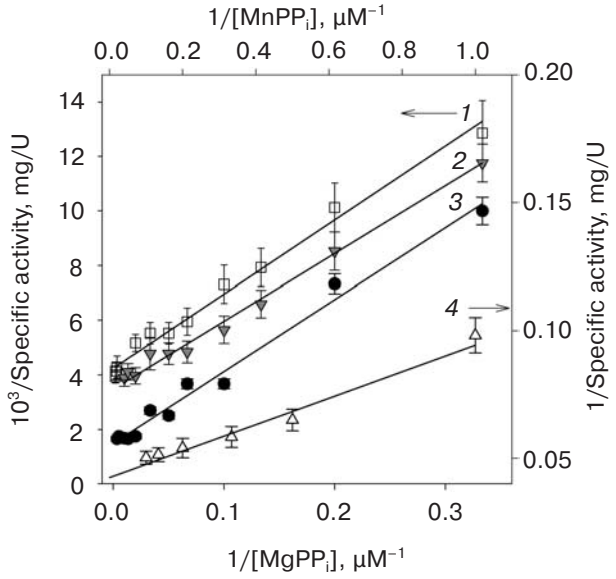

Fig. 1. Mg^{2+}-supported (left and bottom axis) or Mn^{2+}-supported (right and top axis) hydrolysis of PP_i by Mt-PPase: *1*) pH 9.0, 2 mM Mg^{2+}; *2*) pH 7.5, 2 mM Mg^{2+}; *3*) pH 6.0, 10 mM Mg^{2+}; *4*) pH 7.5, 200 μM Mn^{2+}.

ions in the active site may affect the structural stability of PPases, whereas binding in the intertrimeric interface may change the enzymatic activity [15, 16]. The goal of this study was to characterize the interaction of Mt-PPase with Mg^{2+} and Mn^{2+} and to determine the possible influence on this interaction of the two histidine residues in the active site of the enzyme.

Preparation of *M. tuberculosis* PPase without insertions. To obtain recombinant Mt-PPase without additional insertions, a vector was used carrying the Mt-PPase gene with the N-terminal sequence of six histidine residues (kindly provided by Prof. R. Lahti, Turku University, Finland). This original vector was modified in such a way that the gene without insertion could be cut out of it, and thus a new vector was obtained to express Mt-PPase without the six-histidine tag. Based on this vector, a construction was developed and a preparation of untagged Mt-PPase was obtained. The target protein was isolated and purified using a protocol developed earlier for E-PPase [10] with some modifications according to the properties of Mt-PPase. Because this enzyme was not a native protein to the host *E. coli* cells, their cytosolic proteases digested Mt-PPase over a few hours of cell growth. To avoid this problem, in a modified protocol a cell culture was grown for a shorter time (3-4 h). This new protocol produced more protein of high purity.

Mg^{2+}- and Mn^{2+}-supported hydrolysis of substrates. For the preparation of untagged Mt-PPase, kinetic parameters were determined for Mg^{2+}- or Mn^{2+}-supported hydrolysis of PP_i (Fig. 1). Hyperbolic kinetics was observed in both cases, the values of K_m and k_{cat} being listed in Table 1. Like that for E-PPase, Mg^{2+} was found to be more efficient as an activator of hydrolysis than Mn^{2+}. On the whole, Mt-PPase had hydrolytic activity 2-2.5 times lower than E-PPase did under the same conditions.

Compared to E-PPase, Mt-PPase obviously has a pH-optimum shifted to the more acid range, as can be seen from kinetic parameters of PP_i hydrolysis determined at pH 7.5 vs. 9.0. The same was found earlier for the 6-His-Mt-PPase [4]. This finding appears to indicate the strong influence of His21 and/or His86 in the active site of Mt-PPase on the environment of catalytic groups and their pK_a values.

An significant difference between Mt-PPase and E-PPase is that the *M. tuberculosis* enzyme retained hyperbolic kinetics at pH 6.0 and 10 mM Mg^{2+} (Fig. 1, curve *3*). Under these conditions, E-PPase showed non-Michaelis kinetics due to the occupation of its allosteric site with a second molecule of PP_i [17]. This was indicated by the non-linearity of a double-reciprocal plot, which was not however found in the case of Mt-PPase. Such a difference may be caused by a different affinity of the two enzymes for the effector PP_i molecule, up to the entire absence of allosteric site in Mt-PPase.

Table 1. Kinetic parameters of Mg^{2+}- and Mn^{2+}-supported hydrolysis of PP_i by Mt-PPase

Conditions	Kinetic parameters			
	Mt-PPase		E-PPase	
	K_m, μM	k_{cat}, sec^{-1}	K_m, μM	k_{cat}, sec^{-1}
pH 6.0, 10 mM Mg^{2+}	18 ± 3	12.7 ± 0.5	non-Michaelis kinetics [17]	
pH 7.5, 2 mM Mg^{2+}	6.0 ± 0.5	90 ± 2	3.2 ± 0.3	230 ± 4
pH 9.0, 2 mM Mg^{2+}	7 ± 1	77 ± 3	1.3 ± 0.2	250 ± 10
pH 7.5, 200 μM Mn^{2+}	0.9 ± 0.2	16 ± 1	–	–
pH 7.5, 1 mM Mn^{2+}	–	–	0.15 ± 0.05	7 ± 1

Table 2. Mg^{2+}- and Mn^{2+}-supported hydrolysis of ATP and PNP by Mt-PPase (50 mM Tris-HCl, pH 7.5, 300 μM MgATP (or MnATP) or 100 μM MgPNP (or MnPNP))

Substrate	Cofactor	Rate of hydrolysis, min^{-1}	
		Mt-PPase	E-PPase
MgATP	2 mM Mg^{2+}	0.3 ± 0.1	0
MnATP	50 μM Mn^{2+}	0.5 ± 0.1	1.8 ± 0.2*
MgPNP	1 mM Mg^{2+}	0.55 ± 0.05	0.69 ± 0.05
MnPNP	50 μM Mn^{2+}	0.48 ± 0.04	0

* Conditions: 50 mM Tris-HCl, pH 7.5, 0.7 mM MnATP [6].

Mg^{2+}- or Mn^{2+}-supported hydrolysis of two other substrates of family I PPases, ATP and PNP, was studied (Table 2). Both are known to be much poorer substrates for PPases than PP_i. Upon hydrolysis of ATP, all known PPases show a high selectivity toward the nature of metal cofactors [18-20]. For example, PPase from baker's yeast *S. cerevisiae* is capable of removing P_i from ATP or ADP only when Zn^{2+}-, Mn^{2+}-, or Co^{2+}-activated, but not when Mg^{2+}-activated [19]. Mn^{2+} but not Mg^{2+} can stimulate hydrolysis of ATP by E-PPase [6, 20]. According to our results presented here, PNP can be hydrolyzed by E-PPase only when Mg^{2+}-activated. Surprisingly, Mt-PPase did not show this high selectivity toward the nature of metal cofactors. Both Mg^{2+} and Mn^{2+} could support hydrolysis of ATP and PNP by this enzyme, and the resulting activities were comparable (Table 2). As it was in the case of PP_i, Mn^{2+}-supported hydrolysis of ATP by Mt-PPase was one order of magnitude slower than by E-PPase, whereas the rates of Mn^{2+}-supported hydrolysis of PNP by the two enzymes were essentially the same.

Dissociation constants of Mt-PPase complexed with Mg^{2+} or Mn^{2+}. The lack of selectivity of the enzyme toward Mg^{2+} and Mn^{2+} as cofactors might be in part explained by changes in the affinity of one of the metal cofactors for the activator binding sites. The very fact of Mt-PPase having a non-zero catalytic activity shows that the metal cofactor ions, both Mg^{2+} and Mn^{2+}, can occupy all the activator binding sites M1-M3. However, it has been earlier found for E-PPase that the exact position of a metal ion may vary considerably within the single binding site [7]. Thus, a possibility could not be ruled out that residues His21 or His86 could contribute alternative ligands to some of the binding sites, in which case the position of a metal ion in this site would be distorted.

To test this supposition, we determined dissociation constants of Mt-PPase complexed with substrate and with Mg^{2+} or Mn^{2+} cofactor. Hydrolytic activity was measured as a function of concentration of Mg^{2+} or Mn^{2+} in the reaction mixture (Fig. 2). The site M1 has the highest affinity for the metal ion, and its occupation is not seen in the dependence. The site M3 is where the metal ion from a substrate molecule is bound, whose concentration is kept fixed in the experiment. Therefore, the bell-shaped profile corresponds to the occupation of two binding sites, activator site M2 and inhibitor site M4. Corresponding dissociation constants K_d(M2) and K_d(M4) are given in Table 3 together with the values of A_0, which shows a potential level of activity without the inhibitor metal ion.

As can be seen from the data of Table 3, both Mg^{2+} and Mn^{2+} have the same affinity for the site M2 of Mt-PPase, as it was for E-PPase. Mt-PPase however shows lower affinity for both cofactors of the inhibitor site M4. The two enzymes also differ in a degree of inhibition at high concentration of the metal cofactors. Inhibition by Mg^{2+}, for example, lowers activity of Mt-PPase to the level of 70%, while E-PPase is inhibited to 30%. According to the structural data, neither His21 nor His86 in Mt-PPase are located immediately near the supposed

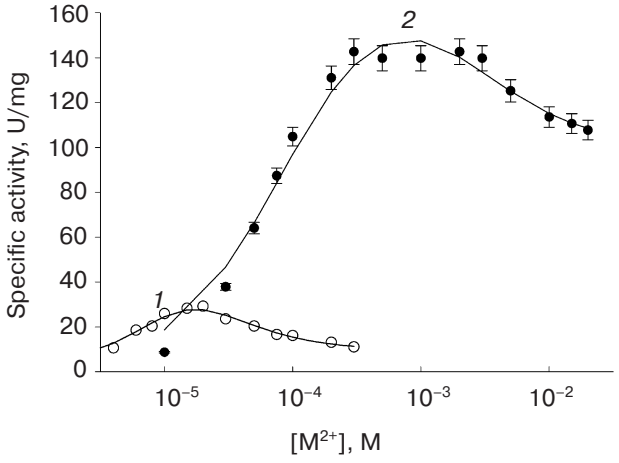

Fig. 2. Hydrolysis of PP_i by Mt-PPase as a function of a metal cofactor (Mn^{2+} (*1*) or Mg^{2+} (*2*)) concentration. PPase was assayed at pH 7.5, 200 μM $MgPP_i$ or 50 μM $MnPP_i$. Lines are the best fit to Eq. (1).

Table 3. Dissociation constants of Mt-PPase complexed with Mg^{2+} or Mn^{2+} determined in the presence of PP_i (parameters are determined from the best fit of data shown in Fig. 2 to Eq. (1))

Enzyme	Cofactor	Parameters		
		K_d(M2), μM	K_d(M4), mM	A_0, U/mg
Mt-PPase	Mg^{2+}	142 ± 41	>35	350 ± 30
E-PPase [20]		200 ± 40	16 ± 2	594 ± 15
Mt-PPase	Mn^{2+}	25 ± 12	0.045 ± 0.020	90 ± 30
E-PPase [6]		25 ± 6	0.029 ± 0.005	1100 ± 50

location of the M4 binding site. At the same time, in the crystal structure of Mt-PPase complexed with SO_4^{2-} (1SXV [4]), the nitrogen atom of the imidazole group of His86 makes direct contact to sulfate ion, which is the analog of a leaving phosphate P_L. This phosphate in the *S. cerevisiae* yeast PPase is in turn one of the direct ligands of the M4 metal ion [21]. In the structure of Mt-PPase complexed with phosphate (1WCF), the side group of His21 contacts via two water molecules with the molecule H_2O 278 whose location is essentially the same as the location of Mn^{2+} in site $M4^P$ in E-PPase [7]. Although the structure of Mt-PPase complexed with the metal ions is still not available, it is not unlikely that in this complex the imidazole groups of both histidine residues are involved in the network of H-bonds immediately around the M4 metal ion. Such an involvement could explain the observed changes in K_d(M4) and the degree of inhibition.

One more difference between the two enzymes is the relative activating efficiency of Mg^{2+} and Mn^{2+}. For Mt-PPase, Mn^{2+}-stimulated activity measured at the maximum is only 20% of that value for Mg^{2+}-stimulated hydrolysis. This fact agrees well with Mt-PPase being an enzyme of family I, which is known to be activated most efficiently by Mg^{2+} rather than Mn^{2+}. It should be noted, that for Mt-PPase the ratio of A_0 values for Mg^{2+}- versus Mn^{2+}-supported hydrolysis is 3.8. In the case of E-PPase, this ratio is 0.54, indicating that for the latter enzyme Mn^{2+} can potentially be more efficient cofactor than Mg^{2+}, but the higher rate of hydrolysis cannot be reached in the experiment due to the tight binding of Mn^{2+} at the inhibitor site M4. Mt-PPase appears to bind the inhibitor metal ion with lower affinity, but even in the absence of inhibition, the activating efficiency of Mn^{2+} is much lower than that of Mg^{2+}.

Generally, Mg^{2+}- and Mn^{2+}-activated Mt-PPase was not found to differ much from the other PPases of family I. Judging from the similarity of the values of K_d(M2) for Mt-PPase and E-PPase (Table 3), residues His21 and His86 are most likely not the direct ligands of metal ion M2. Concerning their participation in the binding of metal ion M4, we cannot make any strict conclusion based on results presented here. The difference observed in the kinetic behavior of Mt-PPase versus E-PPase, particularly in the rates of Mg^{2+}- and Mn^{2+}-supported hydrolysis of their substrates, shows that the imidazole groups have a strong influence on the properties of catalytic groups and charge distribution in the active site.

pH- and metal cofactor-dependent stability of oligomeric structure of Mt-PPase. Prokaryotic PPases of family I are most active as homohexamers. For the *E. coli* enzyme, an ionic pair His-Asp plays a key role in maintaining the intersubunit contact. Destruction of this pair at low pH causes dissociation of hexameric E-PPase to trimers [22]. Magnesium ions are also known to stabilize hexameric E-PPase by occupying three symmetry-related binding sites at the intertrimeric interface. Each of these intertrimeric Mg^{2+} ions makes contacts with protein ligands via water molecules [23]. The sequence of Mt-PPase lacks the amino acid residues identical to these protein ligands, but there is still a possibility of Mg^{2+} binding at the intertrimeric interface. One of the goals of this work was to elucidate the question of whether or not metal cofactor ions, either Mg^{2+} or Mn^{2+}, participate in stabilization of hexameric Mt-PPase.

Stability of the Mt-PPase hexameric form was characterized by hydrolytic activity of the enzyme preparation after its incubation at various fixed pH values. Figure 3 shows pH-dependence of stability of the hexameric PPase incubated without metal ions (curve *1*) or in the presence of either Mg^{2+} (curve *2*) or Mn^{2+} (curve *3*). Oligomeric forms were supposed to differ in their activities, so that the level of remaining activity at each pH would after equilibration be determined by their concentrations in the mixture. For example, for E-PPase the relative activities of the hexameric, trimeric, and dimeric forms are 100, 40, and 10%, whereas the monomeric form appears to be inactive [24]. As can be seen from Fig. 3, the remaining activity of Mt-PPase drops to zero after incubation at pH below 5.0 or above 10.0. It is unusual compared to the enzyme from *E. coli*, which retained 40% activity (trimeric form [24]) after incubation at pH below 5.0, and there is no data on its dissociation at alkali pH.

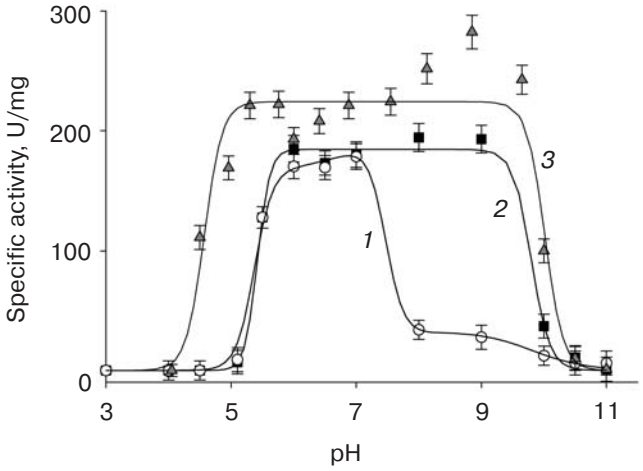

Fig. 3. The pH-dependent stability of hexameric Mt-PPase. Enzyme (6.5 μM) was incubated at fixed pH for 2 h at 25°C in the absence of metal cofactors (*1*) or in the presence of 2 mM Mg^{2+} (*2*) or 100 μM Mn^{2+} (*3*). Activity was assayed in 50 mM Tris-HCl, pH 7.5, at 2 mM Mg^{2+} and 50 μM $MgPP_i$. Lines are the best fit to Eq. (2).

According to the data of velocity sedimentation, Mt-PPase is hexameric at pH 7.0 (s^w_{20} = 7.92 S) and dissociates at pH 4.0 or 10.0 forming monomers (s^w_{20} = 1.46 S) rather than trimers, as is typical for E-PPase. At pH 9.0, in the solution of apoenzyme there is a trace amount of monomer, but the major oligomeric form (s^w_{20} = 5.5 S) appears to be trimer, which is in a good agreement with the non-zero level of hydrolytic activity at pH 8-10. Thus, the additional transition at the alkali pH range was included into the calculation of the corresponding theoretical line (*1*) in Fig. 3. If Mt-PPase was incubated in the presence of metal ions (Mg^{2+} or Mn^{2+}), there was no similar transition observed on the pH-dependence. In this case, sedimentation data show that the enzyme is hexameric up to pH 9.0 and dissociates to monomers at the higher pH. These results indicate that Mg^{2+} and Mn^{2+} can both shift the trimer–hexamer equilibrium, observed for the apoenzyme at pH 8-10, towards the hexameric form. This stabilization may be due to some of the metal ions binding at the active site. It is possible, however, that there is also a binding site at the intertrimeric interface of Mt-PPase, where the metal ions can contact simultaneously with two protein subunits, thus making their interaction stronger.

Unusual character of the pH-dependent dissociation observed here appears to be due to the fact, that the polypeptide chain of Mt-PPase lacks the first 12 amino acid residues at the N-terminus compared to the other bacterial PPases. Analysis of the crystal structure of Mt-PPase shows that due to this feature, some elements of a secondary structure forming intertrimeric interface in E-PPase, in Mt-PPase form intratrimeric interface instead. Another difference is that the intersubunit contacts in Mt-PPase are controlled largely by ionic pairs, which present a much greater part of the total interaction compared to E-PPase (Table 4). As a result, intersubunit interactions inside each trimer are significantly tighter, while interactions between trimers are much weaker in Mt-PPase. These peculiarities of Mt-PPase suggests that the loss of an ionic intertrimeric contact at both low and high pH values causes the highly cooperative destruction of intratrimeric interactions, and thus the hexameric Mt-PPase dissociates directly to monomers. This supposition is in good agreement with the high value of coefficient *m*, which defines the cooperativity of an oligomeric transition (Table 5). For the *E. coli* enzyme, *m* = 2 [4].

From the data shown in Fig. 3, the values of pK_a were determined for the protein groups controlling oligomeric transitions observed in Mt-PPase (Table 5). For the hexamer–monomer transition, the value of pK_a ($pK_a(1)$ = 5.4 in Table 5) is close to that found for the hexamer–trimer transition in E-PPase [22]. This pK_a appears to belong to the conservative ion pair Asp128–His121 of Mt-PPase, which controls the intertrimeric interaction (see Table 4). From the alkali branch of the pH-dependence, the values of constant $pK_a(2)$ can be determined that in a holo-form of Mt-PPase correspond to the hexamer–monomer tran-

Table 4. Intersubunit interactions (ion pairs and H-bonds) within hexameric Mt-PPase and E-PPase based on their crystal structures (pairs of atoms are listed with interatomic distances less than 3.3 Å; ion pairs are given in bold)

Mt-PPase	E-PPase
Inside trimers	
Asp4 Oδ1 – Arg27 NH_2 1	Tyr30 OH – Gln80 NH
Asp4 Oδ2 – Arg27 NH_2 2	Ser36 OH – Ser1Oγ
Thr6 Oγ – Arg25 NH_2 1	Leu39 O – Val84 NH
Ala37 NH – Pro35 O	Val41 NH – Val84 O
Glu46 Oε – Arg25 NH_2 2	Phe44 NH – Leu113 O
Gln64 Nε2 – Gln31 Oε1	Symmetry mirrored pairs
Pro65 O – Asn15 Nδ2	
Leu71 NH – Val26 O	
Leu71 O – Leu28 NH	
Arg 101 NH_2 1 – Tyr 31 O	
Symmetry mirrored pairs	
Between trimers	
Asp128 Oδ2 – His121 Nε2	Asn24 Nδ2 – Asp26 Oδ1
Symmetry mirrored pairs	Ser46 O – Gln133 Nε2
	Ala48 O – Phe50 NH
	His136 Nε2 – Asp143 Oδ2
	Symmetry mirrored pairs

Table 5. The pH-dependent stability of hexameric Mt-PPase (parameters are determined from the best fit of data shown in Fig. 3 to Eq. (2))

Metal ions in incubation mixture	Parameters					
	A_{max} (hexamer), U/mg	A_{max} (trimer), U/mg	pK_a(1)	pK_a(2)	pK_a(3)	m
–	167 ± 5	34 ± 2	5.4 ± 0.1	9.8 ± 0.1	7.5 ± 0.1	4.3 ± 1.5
2 mM Mg^{2+}	185 ± 5	–	5.4 ± 0.1	9.8 ± 0.1	–	4.3 ± 1.3
0.1 mM Mn^{2+}	224 ± 7	–	4.6 ± 0.1	10.0 ± 0.1	–	3.0 ± 1.0

sition. In the apo-form of Mt-PPase, the same constant corresponds to the trimer–monomer transition. The values of pK_a(2) for the cases of dissociation of a hexameric vs. trimeric form to monomers are essentially the same (Table 5), which suggests that these transitions may be controlled by the same protein groups involved in the interaction inside trimers. This value most likely corresponds to a guanidine group of one of the two arginine residues, Arg25 or Arg27, forming intratrimeric ion pairs. In addition, only in the case of the apo-enzyme an intermediate transition, hexamer–trimer, was found at alkali pH, with the corresponding acidity constant pK_a(3). This constant most likely belongs to the imidazole group of His125, whose protonation may be yet another factor controlling the stability of ion contact Asp128–His121, as found in E-PPase [22].

The most interesting feature of Mt-PPase compared to all other PPases of family I is that there are two histidine residues in the active site of this enzyme in immediate proximity to the binding sites for the cofactor metal ions. Due to a high evolutionary conservativeness of the active site in pro- and eukaryotic PPases, it was not a very promising idea so far to use these enzymes as targets for the design of antibacterial agents. Now that Mt-PPase is found with this unique feature that distinguishes it from the eukaryotic enzymes including human PPase, this enzyme becomes a very promising object for developing its specific inhibitors. Histidine residues are known to form many tight complexes in proteins, including that with divalent metal ions, especially with Mg^{2+}, Mn^{2+}, and Zn^{2+}. Therefore, histidine residues in the active site of Mt-PPase could cause this enzyme to change its metal cofactor specificity.

From the results presented here, it can be concluded that His21 and His86 are unlikely to make direct contacts with the metal cofactor ions. However, two imidazole groups in the active site of Mt-PPase, with their nucleophilic and complexing potential, affect greatly the microenvironment of the catalytic groups. As a result, this enzyme lacks that fine tuning for the particular metal cofactor typical for E-PPase and for the other PPases of family I. This can be seen from decreased Mg^{2+}-supported hydrolytic activity and from the similarity of the catalytic properties of Mg^{2+}- or Mn^{2+}-activated enzyme. Mt-PPase is still the only known PPase with the close parameters of Mg^{2+}- vs. Mn^{2+}-supported hydrolysis of its substrates. Due to this difference between Mt-PPase and the other PPases of family I, further study of this enzyme seems to be of high interest from the point of view of finding its specific inhibitors, which could be a basis for new anti-tuberculosis agents.

The authors thank Prof. R. Lahti (Turku University, Finland) for kindly providing us with the original plasmid of 6His-Mt-PPase.

This work was financially supported by the Russian Foundation for Basic Research (grant No. 06-04-49127).

REFERENCES

1. Smith, I. (2003) *Clin. Microbiol. Rev.*, **16**, 463-496.
2. Vijayan, M. (2005) *Tuberculosis (Edinb.)*, **85**, 357-366.
3. Goulding, C. W., Apostol, M., Anderson, D. H., Gill, H. S., Smith, C. V., Kuo, M. R., Yang, J. K., Waldo, G. S., Suh, S. W., Chauhan, R., Kale, A., Bachhawat, N., Mande, S. C., Johnston, J. M., Lott, J. S., Baker, E. N., Arcus, V. L., Leys, D., McLean, K. J., Munro, A. W., Berendzen, J., Sharma, V., Park, M. S., Eisenberg, D., Sacchettini, J., Alber, T., Rupp, B., Jacobs, W., Jr., and Terwilliger, T. C. (2002) *Curr. Drug Targets Infect. Disord.*, **2**, 121-141.
4. Tammenkoski, M., Bellini, S., Magretova, N. N., Baykov, A. A., and Lahti, R. (2005) *J. Biol. Chem.*, **280**, 41819-41826.
5. Salminen, A., Ilias, M., Belogurov, G. A., Baykov, A. A., Lahti, R., and Young, T. (2006) *Biochemistry (Moscow)*, **71**, 978-982.
6. Vainonen, Yu. P., Rodina, E. V., Vorobyeva, N. N., Kurilova, S. A., Nazarova, T. I., and Avaeva, S. M. (2001) *Russ. Chem. Bull.*, **50**, 1877-1884.
7. Samygina, V. R., Moiseev, V. M., Rodina, E. V., Vorobyeva, N. N., Popov, A. N., Kurilova, S. A., Nazarova, T. I., Avaeva, S. M., and Bartunik, H. D. (2007) *J. Mol. Biol.*, **366**, 1305-1317.
8. Merckel, M. C., Fabrichniy, I. P., Salminen, A., Kalkkinen, N., Baykov, A. A., Lahti, R., and Goldman, A. (2001) *Structure*, **9**, 289-297.

9. Halonen, P., Tammenkoski, M., Niiranen, L., Parfenyev, A. N., Goldman, A., Baykov, A., and Lahti, R. (2005) *Biochemistry*, **44**, 4004-4010.
10. Oganessyan, V. Yu., Kurilova, S. A., Vorobyeva, N. N., Nazarova, T. I., Popov, A. N., Lebedev, A. A., Avaeva, S. M., and Harutyunyan, E. G. (1994) *FEBS Lett.*, **348**, 301-304.
11. Josse, J. (1966) *J. Biol. Chem.*, **241**, 1938-1947.
12. Baykov, A. A., and Avaeva S. M. (1981) *Analyt. Biochem.*, **116**, 1-4.
13. Perrin, D. D. (1979) *Stability Constants of Metal–Ion Complexes* (IUPAC Chemical Data Series, No. 22), Pergamon Press, Oxford.
14. Smirnova, I. N., Baykov, A. A., and Avaeva, S. M. (1986) *FEBS Lett.*, **206**, 121-124.
15. Vorobyeva, N. N., Nazarova, T. I., Bakuleva, N. P., Avaeva, S. M., Protasevich, I. I., and Platonov, A. L. (1982) *Biokhimiya*, **47**, 740-745.
16. Baykov, A. A., Hyytia, T., Volk, S. E., Kasho, V. N., Vener, A. V., Goldman, A., Lahti, R., and Cooperman, B. S. (1996) *Biochemistry*, **35**, 4655-4661.
17. Sitnik, T. S., Vainonen, J. P., Rodina, E. V., Nazarova, T. I., Kurilova, S. A., Vorobyeva, N. N., and Avaeva, S. M. (2003) *IUBMB Life*, **55**, 37-41.
18. Kurilova, S. A., Bogdanova, A. V., Nazarova, T. I., and Avaeva, S. M. (1984) *Bioorg. Khim.*, **10**, 1147-1151.
19. Cooperman, B. S. (1982) *Meth. Enzymol.*, **87**, 526-548.
20. Rodina, E. V., Vainonen, Y. P., Vorobyeva, N. N., Kurilova, S. A., Nazarova, T. I., and Avaeva, S. M. (2001) *Eur. J. Biochem.*, **268**, 3851-3857.
21. Zyryanov, A. B., Pohjanjoki, P., Kasho, V. N., Shestakov, A. S., Goldman, A., Lahti, R., and Baykov, A. A. (2001) *J. Biol. Chem.*, **276**, 17629-17634.
22. Velichko, I. S., Mikalahti, K., Kasho, V. N., Dudarenkov, V. Y., Lahti, R., and Baykov, A. A. (1998) *Biochemistry*, **37**, 734-740.
23. Kankare, J., Salminen, T., Lahti, R., Cooperman, B. S., Baykov, A. A., and Goldman, A. (1996) *Biochemistry*, **35**, 4670-4677.
24. Vainonen, Ju. P., Kurilova, S. A., and Avaeva, S. M. (2002) *Bioorg. Khim.*, **28**, 426-433.